Desalination, 85 (1991) 33–44
Elsevier Science Publishers B.V., Amsterdam – Printed in The Netherlands

The Effects of Small Halocarbons on RO Membrane Performance

R. CHENG[1], J. GLATER[2], J.B. NEETHLING[3] and M.K. STENSTROM[2]

[1]*Metropolitan Water District of Southern California, La Verne, CA (USA)*
[2]*Civil Engineering Department, University of California, Los Angeles, CA (USA)*
[3]*HDR Engineering, Inc., El Dorado Hills, CA (USA)*

(Received March 31, 1991)

SUMMARY

The effects of small halocarbons, $CHCl_3$, $CHBr_3$ and CCl_4, at 50 mg/l concentrations on the performance of three typical RO membranes were examined. Cellulose acetate, polyamide and advanced composite membranes were used in this study. The flux, total dissolved solids (TDS) rejection, halocarbon rejection, partition coefficient and void volume tests were conducted to evaluate the effects of halocarbon addition. In general, the halocarbons were poorly rejected by all three membranes. This was accompanied by increased rates of flux decline and increased TDS rejection over controls without halocarbons. Partition tests revealed the advanced composite membrane adsorbed all three test halocarbons much more strongly than either cellulose acetate or polyamide membranes. The strong affinity for halocarbons must be considered when using the advanced composite membrane for various waste water applications.

SYMBOLS

F_t — water flux at time t (gal/ft^2–d (GFD))
K — membrane constant (GFD)
K_s — organic distribution coefficient (unitless)
m — log-log flux decline index (unitless)
Q — amount of permeate per unit area membrane (gal/ft^2)
t — time (days)
t_0 — initial time (days)
w_d — weight of dry membrane (g)
w_w — weight of wet membrane (g)

0011-9164/91/$03.50

Greek

ε — dielectric constant of medium (C/V-cm)
ε_v — membrane void fraction (unitless)
ρ_d — density of dry membrane (g/cm^3)
ρ_e — density of wet membrane (g/cm^3)

INTRODUCTION

RO applications have recently expanded to areas as diverse as municipal, agricultural and industrial waste water reclamation as well as the production of ultrapure waters in the semiconductor industry. With these applications, new foulants such as organic materials are encountered. One class of organics which is of interest to the RO industry but has not been sufficiently studied is small halocarbons such as chloroform and bromoform, which are often encountered as disinfection by-products.

Research at the Yuma desalting facility plant (Yuma) in Yuma, Arizona, detected the presence of these constituents in their influent waters. The Yuma facility is the world's largest for desalting irrigation water utilizing RO. Several authors [1,2] have speculated that membrane interactions with halocarbons, other dissolved organics, and colloidal matter are responsible for the rapid flux decline observed during early tests at the Yuma facility. Membrane fouling problems have delayed the opening of this important membrane plant. The research reported herein addresses membrane/halocarbon interactions.

EXPERIMENTAL

Three DuPont membranes were used in this study: cellulose acetate (7460 CA), aromatic polyamide (5930 B9 (PA)), and an advanced composite or thin film (89006 ACM). The experimental once-through RO system used for membrane testing is shown in Fig. 1. The driving pressure was 400 psi, which simulated the operating pressure at Yuma. The feed water quality was approximately 200–220 mg/l TDS.

Twelve sets of experiments of approximately 125 h each were conducted in this study. Each membrane type was tested without halocarbons and with each of the following halocarbons: $CHCl_3$, $CHBr_3$ and CCl_4. CCl_4 was selected as a representative nonpolar compound to contrast with $CHCl_3$ and $CHBr_3$, which are polar. In each experiment the total product volume and TDS and halocarbon concentrations of the influence and effluent were measured. Controls were run with untreated tap water.

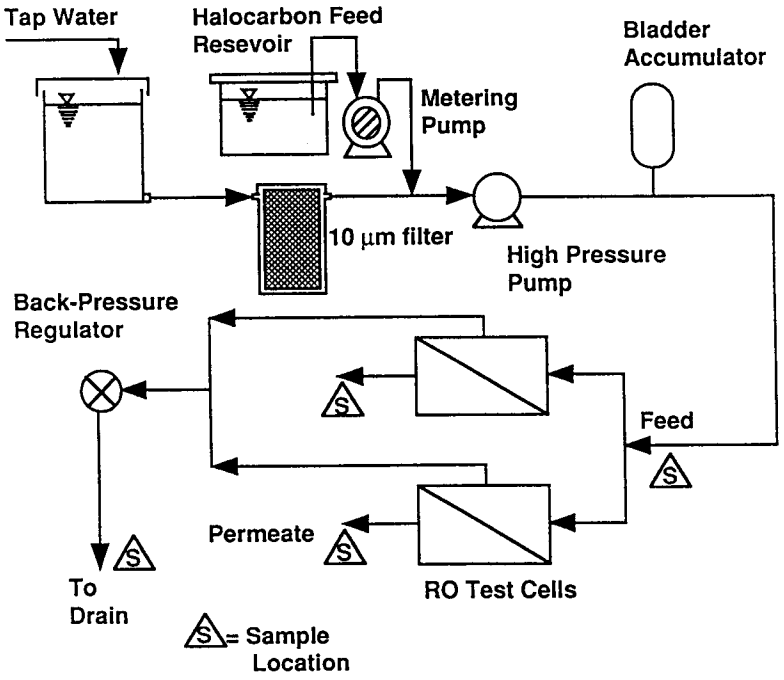

Fig. 1. Schematic diagram of one-pass RO test unit.

TDS measurements were conducted by using a YSI model 35 conductance meter with a model 3403 probe (cell constant of 1 cm^{-1}). Halocarbon detection was performed using a Varian/Tekmar model 00-996367-00 purge and trap concentrator with trap material made of Tenax, silica gel and charcoal. The concentrator was attached to a Hewlett-Packard (HP) model 5890 gas chromatograph (GC) equipped with a flame-ionization detector. The capillary column used was a J&W DB-624 liquid phase silica column. The time and temperature program used for the purge and trap concentrator was set as follows: 11 min purge at 30°C, 4 min desorb at 180°C and 8 min bake time at 180°C. The GC time and temperature program settings were as follows: 35°C initial temperature, 140°C final temperature, 4 min initial hold time, 1 min final hold time and 8°C/min temperature program. The GC and purge/trap gas flow rates were: helium carrier gas at 5.58±0.07 ml/min, hydrogen combustion gas at 47.2±0.7 ml/min and dry air purge gas at 315±4 ml/min. Output from the GC was integrated using an HP model 3392A integrator.

Static soak tests designed to measure the partitioning of the halocarbons between membrane phase and the solution phase, designated by the parameter K_s, were performed on the three membranes. The solutions contained the following halocarbon concentrations: 0, 50, 100, 250, 500, 1000

and 2000 mg/l. This test was modified from a previously developed procedure by Pusch et al. [3]. Two membrane samples were placed in each solution for 10 d to allow steady-state to occur. After this period both pieces were removed from solution, rinsed with DI water and blotted dry. One piece was used for halocarbon extraction and the other used for void volume determinations. The extraction was performed by soaking the membrane in trimethylphosphate (TMP), collecting an aliquot of the TMP and diluting with DI water, and injecting this diluted sample into the purge and trap/GC. Results from the soak tests were subsequently used to calculate the membrane/water partition coefficient for each halocarbon.

The void volume test [4] measures the percentage of membrane voids (ε_v). After the membranes were soaked for 10 d and subsequently rinsed and blotted, the thickness was determined. Afterwards, the wet membranes were placed in a drying oven at 104°C for 4 d and the thicknesses remeasured. Results of this test were used for comparing the effects of different halocarbon concentrations on the membrane void fractions.

MODELLING MEMBRANE PERFORMANCE

Merten's unsteady-state flux equation modified for volume calculations [5] is as follows:

$$F_t = Kt^m \tag{1}$$

which after integrating over time becomes:

$$Q = \frac{K}{m+1}\left(t^{m+1} - t_0^{m+1}\right) \tag{2}$$

If t_0 is assumed to be zero, Eqn. (2) can be rearranged as follows:

$$\log Q = \log\left(\frac{K}{m+1}\right) + (m+1)\log(t) \tag{3}$$

This equation may be used to calculate the coefficient m and the constant K. When these values are replaced into Eqn. (1), the flux at any time t may be generated.

The uptake of halocarbons by the membranes is measured by the parameter K_s, which is defined as:

$$K_s = \left(\frac{\text{mole organic in membrane phase}}{\text{kg wet membrane}}\right) \Big/ \left(\frac{\text{mole organic in solution phase}}{\text{kg solution}}\right) \tag{4}$$

The membrane void fraction ε_v is defined by the following equations:

$$\varepsilon_v = \frac{\Delta V}{1+\Delta V} \tag{5}$$

$$\Delta v = \frac{\rho_d (w_w - w_d)}{\rho_e w_d} \tag{6}$$

ε_v may be thought of as the ratio of void volume in a membrane sample to the total membrane volume. If total membrane volume remains relatively constant over the course of an experiment, then any changes in ε_v may be attributed to changes in void volume. An increase in ε_v indicates an increase in void volume, and the converse is also true.

RESULTS AND DISCUSSION

Fig. 2 shows the results from the product volume experiment for DuPont's AC membrane. The lines in this figure were calculated using Eqn. (2). In each case the experimental data and the predictions are in good agreement, giving correlation coefficients of 0.999 or above. The halocarbon addition decreased the membrane flux since all product volume lines are below the baseline volume. The CCl_4 and $CHCl_3$ tests were conducted for 170 h since tests were also conducted for fouling reversibility. At the end of 125 h, the halocarbon feed pump was shut off and the product water volume was measured.

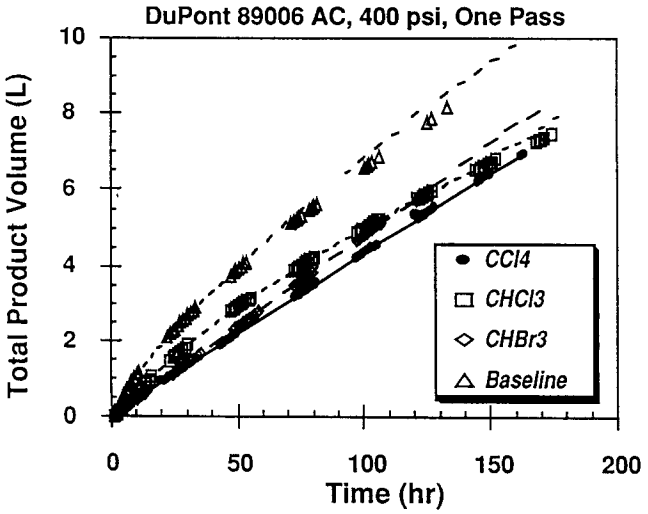

Fig. 2. Total product volume vs. time for DuPont 89006 AC membrane (broken lines show best fit from Eqn. (3)).

Tests using $CHCl_3$, $CHBr_3$ and CCl_4 yielded product water volumes of 5.91±0.08, 5.88±0.09 and 5.43±0.08 L, respectively. The baseline product water volume was 7.81±0.98 L. $CHCl_3$ and $CHBr_3$ caused approximately 25% decrease in the AC membrane's flux while CCl_4 caused a 31% decrease. Flushing the membranes with tap water did not restore product flux. This flux decline may either be reversible or irreversible since leaching out all of the sorbed organic may take much more time than what was given for flushing.

Fig. 3 shows the percent change from baseline product water volumes upon halocarbons addition after 125 h operation. The CA membrane appeared to be affected the least by halocarbon addition, while AC was affected the most by halocarbon addition. $CHBr_3$ and $CHCl_3$ decreased PA and AC membranes' flux from baseline almost equally at 20%.

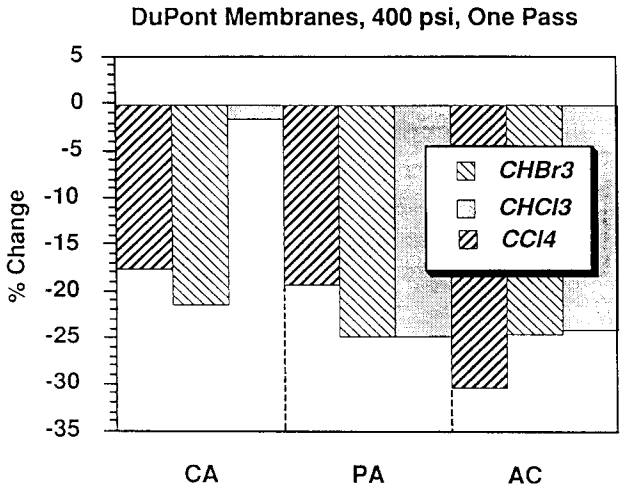

Fig. 3. Percent change from baseline product water volume for CA, PA and AC membranes.

Fig. 4 compares TDS rejection for the three membranes at the end of the test period. CA showed the best baseline TDS rejection followed by PA and AC membranes. Halocarbon addition improved TDS rejection slightly for CA membrane, ranging from 1 to 1.5% increase, while AC membrane's TDS rejection characteristic improved by 4 to 8%. Additions of both $CHBr_3$ and CCl_4 decreased PA's TDS rejection capabilities.

Fig. 5 shows average halocarbon rejection for the three membranes. CA showed the worst halocarbon rejection with a maximum average rejection for CCl_4 of 32%. PA rejected CCl_4 by approximately 60%. The AC membrane showed the best halocarbon rejection at 38% for $CHCl_3$ and 83% for CCl_4. In each case $CHCl_3$ was rejected the least and CCl_4 was rejected the most

by each membrane. This observation supports the idea that in general, rejection of these organic molecules is inversely related to size.

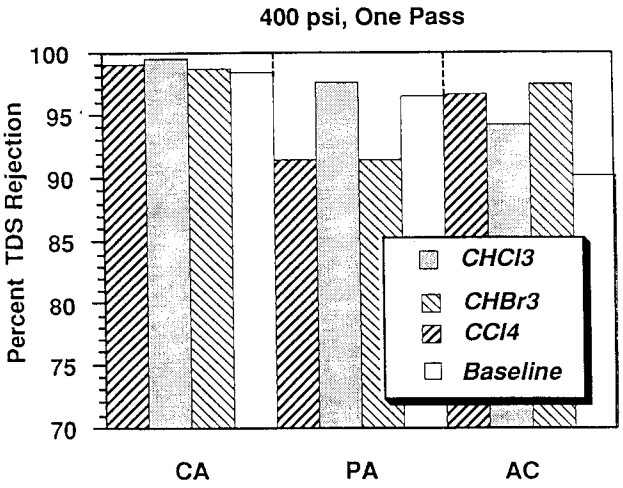

Fig. 4. TDS rejection at 125 h for CA, PA and AC membranes.

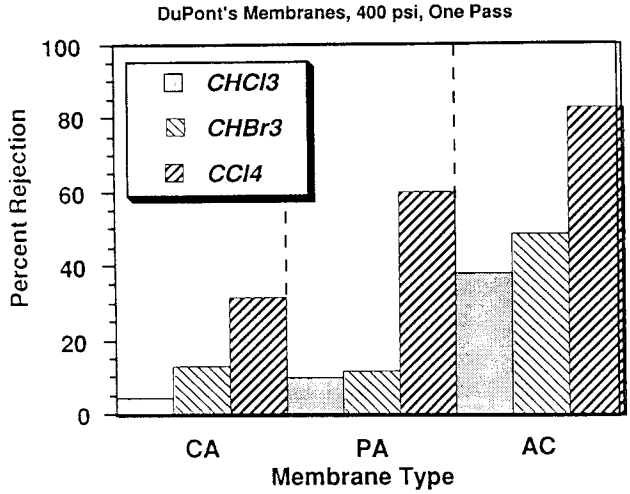

Fig. 5. Average halocarbon rejection for CA, PA and AC membranes.

Fig. 6 shows TDS rejection vs. time data for the AC membrane. While no equilibrium value was reached in this series of experiments, the halocarbons generally improved the membrane's rejection capability. At the end of 125 h, TDS rejection for $CHBr_3$, CCl_4, $CHCl_3$ and baseline cases were $97.5 \pm 0.2\%$, $96.6 \pm 0.2\%$, $94.3 \pm 0.2\%$ and $90.3 \pm 0.3\%$. These data, combined with volume data from Fig. 2, suggested membrane swelling within the AC membrane.

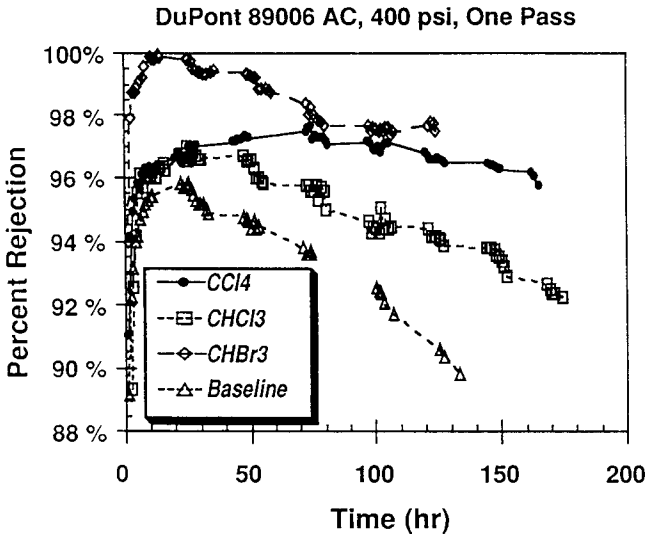

Fig. 6. TDS rejection vs. time for AC with halocarbon addition.

Fig. 7 shows halocarbon rejection vs. time data for the AC membrane. Although data scatter is evident, the average values obtained for CCl_4, $CHBr_3$ and $CHCl_3$ were 80.3 ± 2.5%, 48.9 ± 1.7% and 36.4 ± 1.3%, respectively. Although the AC membrane rejected halocarbons better than either CA or PA membranes, the order of halocarbon rejection was the same for all three membranes: CCl_4 > $CHBr_3$ > $CHCl_3$. This appears to be consistent with the size and polarity of these compounds.

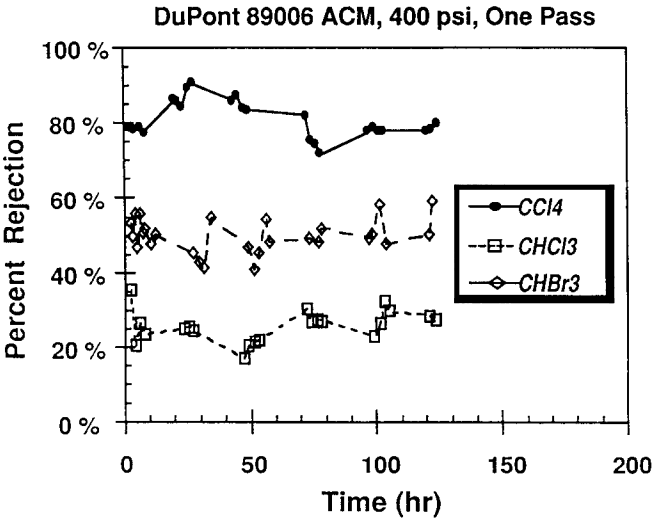

Fig. 7. Halocarbon rejection vs. time for DuPont 89006 AC membrane.

Fig. 8 presents the partition coefficient K_s vs. halocarbon concentration data collected in soak tests using DuPont's AC membrane. Halocarbons partitioned more strongly into the AC membrane than into CA or PA membranes. No concentration independent region existed with K_s; for comparison purposes we used the average values above 500 mg/l halocarbon concentration. The values for $CHCl_3$, $CHBr_3$ and CCl_4 were 2.49± 0.23, 1.82±0.29 and 0.72±0.06. These data indicated that $CHCl_3$ partitions 27% more than $CHBr_3$ and 71% more than CCl_4 into the AC membrane.

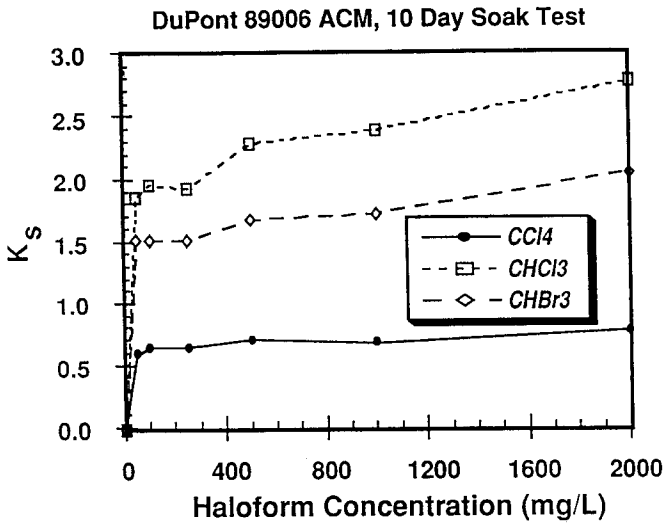

Fig. 8. K_s vs. halocarbon concentration for DuPont's AC membrane.

Fig. 9 shows a comparison between the K_s values for the three halocarbons with the DuPont CA, PA and AC membranes at a halocarbon concentration of 2000 mg/l. This graph shows that the AC membrane adsorbed halocarbons more strongly than either CA or PA membranes. CA and PA membranes adsorbed halocarbons almost to the same extent.

Fig. 10 show the results obtained from the void fraction vs. halocarbon concentration tests. If the change in the total membrane is small compared to the change in the membrane voids, then any increases or decreases in the parameter (ε_v) may be attributed solely to either increases or decreases in the membrane void volume.

This figure shows all three membranes' void fractions decreased with halocarbon addition. A rough comparison between the void fraction at 0 mg/l and 2000 mg/l halocarbon addition showed the percentage decreases for AC, CA and PA membranes to be 50%, 40% and 23%, respectively. This indicated AC membrane void fraction was reduced the most by halocarbon addition while PA's void fraction was reduced the least. This trend parallels the pattern shown in the halocarbon partition experiments where the AC

membrane adsorbed the greatest amount of halocarbon and PA and CA adsorbed less.

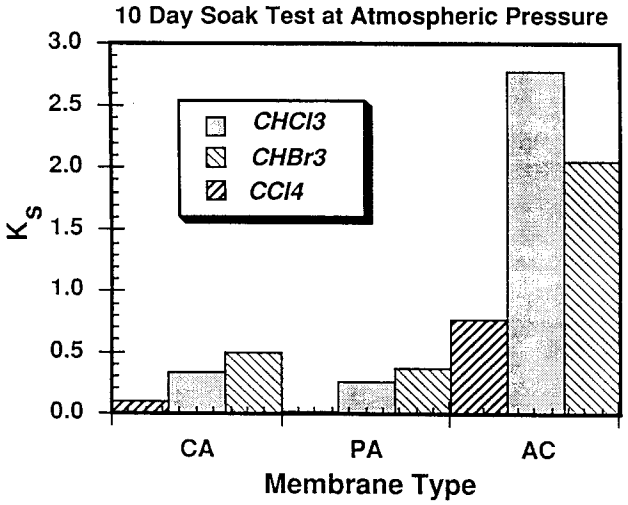

Fig. 9. Comparison of K_s among membranes.

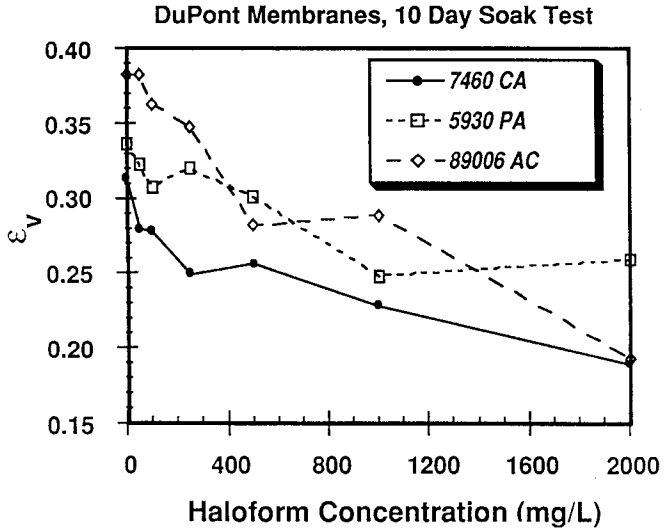

Fig. 10. Void fraction vs. halocarbon concentration.

Fig. 11 shows the relationship between dielectric constant and percent organic rejection using DuPont's CA membrane. The data for $CHBr_3$ and $CHCl_3$ were obtained in this study; the other data were obtained from the literature [6]. This figure shows that as a compound's dielectric constant increases (i.e., becomes a poorer insulator), its rejection by the membrane decreases. This figure also shows that organic rejection is not solely dependent on molecule size.

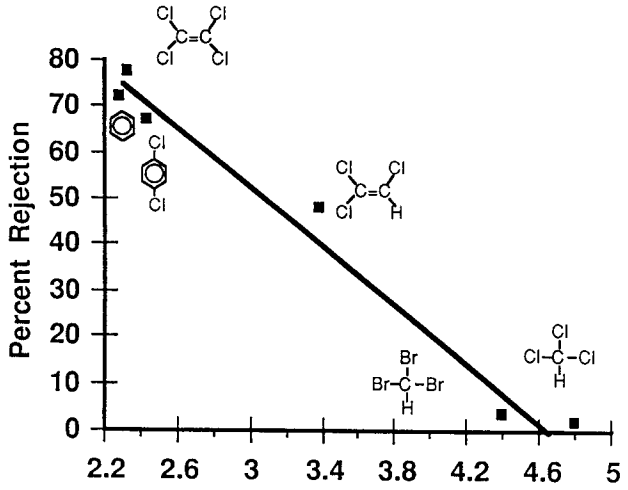

Fig. 11. Dielectric constant, ε vs. percent projection.

CONCLUSIONS

We found the higher flux membranes such as the thin-film type (ACM) experienced a faster decline in performance than lower flux membranes such as the CA type when exposed to the same feed waters containing halocarbons. The TDS rejection increased slightly with all membranes. These observations support the hypothesis that the halocarbons enter the membrane structure and cause a reduction in the void spaces through which water and dissolved solids pass.

The results from the halocarbon partition tests showed that the small organic halocarbons used in this study partition much more strongly into the AC membrane than either CA or PA membranes. These experiments show that smaller halocarbons such as $CHCl_3$ partition into membranes to a greater extent than larger molecules such as CCl_4. Also, more polar compounds are less likely to be rejected than less polar compounds.

Void volume tests demonstrated halocarbon addition under atmospheric pressure conditions caused membrane void spaces to "tighten up". In each experiment with the different membranes, we found there was a reduction in the membrane void volume with an increase in halocarbon concentration. The addition of halocarbons affected the AC membrane void fractions the most.

While the AC membrane was affected the most by halocarbon addition, it also rejected halocarbons to the greatest extent. This may be attributed in part to the pore volume of the AC membrane which is smaller than that of the PA and CA membranes. Halocarbon partition tests indicate the halocarbons may not actually be rejected but adsorbed by the membrane.

All these observations lead to one general conclusion: although the AC membrane has a higher flux than either the CA or PA membranes, its sensitivity to halocarbons suggests caution when considering it for treating feed waters containing these organic compounds.

ACKNOWLEDGEMENTS

The authors are indebted to Dr. Irving Moch of E.I. DuPont Company and Brian Smith of the California Department of Water Resources for their help and guidance on this project. This project was partially funded by the California Department of Water Resources (Contract B55037) and the E.I. DuPont Company (Contract D881130).

REFERENCES

1 J.W. Kaakinen and C.D. Moody, ACS Symposium Series No. 281: Reverse Osmosis and Ultrafiltration, 1985, p. 359.
2 J. Glater, L.C. Wilson and J.B. Neethling, Advances in Chemistry Series No. 281: Aquatic Humic Substances: Influence on Fate and Treatment of Pollutants, 1989, p. 783.
3 W. Pusch, H.G. Burghoff and E. Staude, 5th Internat. Symposium on Fresh Water from the Sea, Athens, 1976, p. 4.
4 P. Pintauro, Mass Transfer of Electrolytes in Membranes, Ph.D. dissertation, University of California, Los Angeles, 1980.
5 R. Weschler, Water Research, 13 (1979) 565.
6 H.W. Pohland, New polyamide composite membranes for ultrapure fluids, Proc., NAMS' 89, Austin, TX, 1989.